

# Journal of Materials Chemistry A

Accepted Manuscript



This is an *Accepted Manuscript*, which has been through the Royal Society of Chemistry peer review process and has been accepted for publication.

*Accepted Manuscripts* are published online shortly after acceptance, before technical editing, formatting and proof reading. Using this free service, authors can make their results available to the community, in citable form, before we publish the edited article. We will replace this *Accepted Manuscript* with the edited and formatted *Advance Article* as soon as it is available.

You can find more information about *Accepted Manuscripts* in the [Information for Authors](#).

Please note that technical editing may introduce minor changes to the text and/or graphics, which may alter content. The journal's standard [Terms & Conditions](#) and the [Ethical guidelines](#) still apply. In no event shall the Royal Society of Chemistry be held responsible for any errors or omissions in this *Accepted Manuscript* or any consequences arising from the use of any information it contains.

Cite this: DOI: 10.1039/c0xx00000x

www.rsc.org/xxxxxx

ARTICLE TYPE

## Benzodithiophene Homopolymers Synthesized by Grignard Metathesis (GRIM) and Stille Coupling Polymerizations

Harsha D. Magurudeniya,<sup>a</sup> Ruvini S. Kularatne,<sup>a</sup> Elizabeth A. Rainbolt,<sup>a</sup> Mahesh P. Bhatt,<sup>a</sup> John W. Murphy,<sup>b</sup> Elena E. Sheina,<sup>c</sup> Bruce E. Gnade,<sup>b</sup> Michael C. Biewer<sup>a</sup> and Mihaela C. Stefan<sup>\*a</sup>

Received (in XXX, XXX) Xth XXXXXXXXX 20XX, Accepted Xth XXXXXXXXX 20XX

DOI: 10.1039/b000000x

Poly{ 4,8-bis(95-dodecylthiophene-2yl)benzo[1,2-*b*:4,5-*b'*]dithiophene } has been synthesized by both Grignard metathesis (**P1**) and Stille coupling polymerizations (**P2**). Polymers **P1** and **P2** were characterized and their optoelectronic properties, charge carrier mobilities, and photovoltaic properties were compared. The field-effect mobilities of the polymers were measured on both untreated and heptadecafluoro-1,1,2,2-tetrahydro-decyl-1-trimethoxysilane (FS) treated OFET devices. The polymers were also evaluated in bulk heterojunction solar cells with [6,6]-phenyl-C71-butyric acid methyl ester (PC<sub>71</sub>BM) as the acceptor.

### Introduction

Due to their good optoelectronic properties and processability, organic semiconducting polymers have been extensively investigated by research communities from both academia and industry.<sup>1-3</sup> Semiconducting polymers have been used in polymer solar cells (PSC), organic field-effect transistors (OFETs), organic light emitting diodes (OLEDs) and in sensors because of their light weight, flexibility and low cost.<sup>1, 4, 5</sup> Among the numerous organic semiconducting polymers that have been synthesized, regioregular poly(3-hexylthiophene) has been the most studied and can be synthesized by McCullough, Rieke and Grignard metathesis (GRIM) polymerization methods.<sup>6-8</sup> Although poly(3-hexylthiophene) exhibits good optoelectronic properties, current research has shifted towards design and synthesis of novel thiophene-based materials with enhanced properties. One such strategy is to synthesize conjugated polymers containing fused ring building blocks.<sup>9</sup> Fused ring thiophene units exhibit rigid backbone structures and greater overlap of the  $\pi$ -conjugated units, both inter and intramolecularly. These features lead to lowering the polymer band gap and increasing the intermolecular interactions in solid films.<sup>10</sup> One of the most extensively studied fused ring thiophene system in the organic electronics field is the benzo[1,2-*b*:4,5-*b'*]dithiophene (BDT).<sup>9, 11-14</sup> Benzodithiophene building block provide high planarity to the polymer backbone. The central benzene core of the fused ring permits the incorporation of different substituents while maintaining its planarity. Moreover, the highest occupied molecular orbital (HOMO) and lowest unoccupied molecular orbital (LUMO) energy levels of the polymers and hence the band gap of the polymers, the absorbance maxima in UV-Vis spectra, and the solubility of the polymers in common organic solvents can be controlled by attaching different substituent to the 4- and 8- positions of the BDT core. Also the symmetric nature of the BDT eliminates the need to

polymerization techniques which allow control of regioregularity during polymerization.<sup>9, 11, 14</sup> Additionally, due to the larger planar conjugated structure of the BDT unit, polymers can easily form  $\pi$ - $\pi$  interactions, which result in high charge carrier mobilities.<sup>11</sup> Due to these structural advantages, many BDT donor-acceptor copolymers with high power conversion efficiencies (PCEs) have been synthesized by varying substituents such as alkoxy, alkyl, alkylthiophene, and alkylbithiophene substituents at 4- and 8- positions of the BDT unit.<sup>12, 14-26</sup> This class of polymers has reached PCE as high as 9.2% in bulk heterojunction (BHJ) solar cells and charge carrier mobilities  $\sim 0.2 \text{ cm}^2 \text{ V}^{-1} \text{ s}^{-1}$  in organic field effect transistors.<sup>27, 28</sup> Almost all these copolymers have been synthesised *via* Stille cross-coupling and Suzuki cross-coupling reactions. These cross coupling reactions resulted in polymers with larger molecular weights, thus limiting the solubility in common organic solvents. Also, due to the *non-living* nature of these coupling reactions, broader polydispersity indices (PDIs) were observed in the polymers. The broader PDIs indicate the presence of low molecular weight polymers, oligomers, and unreacted monomers and by products in the polymer mixtures, which may decrease the BHJ solar cells and OFETs device performances.<sup>29, 30</sup> Therefore it is of tremendous importance to utilize different polymerization techniques for the synthesis of D-A copolymers as well as for homopolymers. A more controlled synthesis and lower PDI can be obtained by a chain growth polymerization technique such as Grignard metathesis (GRIM) polymerization which has been extensively used for the synthesis of regioregular P3HT.<sup>31, 32</sup> GRIM is a quasi-*living* nickel-initiated cross-coupling polymerization technique which generates regioregular P3HT with well-defined molecular weights and narrow PDIs.<sup>31, 32</sup> Moreover, GRIM method allows the polymerization to occur at room temperature.<sup>31</sup> However, the use of GRIM polymerization technique for polymerization of bulky donor monomers has not

been extensively studied.<sup>33-36</sup> Our group recently reported the synthesis of a bulky donor polymer, fused benzodithiophene with phenylethynyl substituent by GRIM polymerization.<sup>14, 36</sup> GRIM polymerization of phenylethynyl substituted benzodithiophene yielded a polymer with a lower molecular weight and a narrow PDI. We speculated that due to the coordination of Ni to the ethynyl linkage of the phenylethynylbenzodithiophene monomer during the catalytic cycle we obtained a polymer with lower molecular weight. Therefore here in this report to overcome the coordination of Ni to the ethynyl linkage, 2-dodecylthiophene has been substituted to the 4- and 8- positions of the benzodithiophene. Thus the synthesized 2,6-dibromo-4,8-bis(5-dodecylthiophene-2-yl)benzo[1,2-*b*:4,5-*b'*]dithiophene was polymerized by GRIM and as a comparison 2,6-dibromo-4,8-bis(5-dodecylthiophene-2-yl)benzo[1,2-*b*:4,5-*b'*] dithiophene was also polymerized *via* Stille coupling polymerization. The two polymers obtained from these two techniques were characterized and their molecular weights, PDI values, charge carrier mobilities and photovoltaic properties were compared.

## Materials and Characterization

All commercial chemicals were purchased from Aldrich Chemicals and were used without further purification unless otherwise noted. All reactions were conducted under nitrogen environment. All the glassware and syringes were dried at 120 °C for at least 24 hrs before use and cooled under a nitrogen atmosphere. Tetrahydrofuran was dried over sodium/benzophenone ketyl and freshly distilled prior to use. 4,8-dihydrobenzo[1,2-*b*:4,5-*b'*]dithiophene-4,8-dione,<sup>37</sup> 2,6-dibromo-4,8-bis(5-dodecylthiophene-2-yl)benzo[1,2-*b*:4,5-*b'*]dithiophene and 2,6-(trimethyltin)-4,8-bis(5-dodecylthiophene-2-yl)benzo[1,2-*b*:4,5-*b'*]dithiophene were prepared according to the literature.<sup>7,24</sup> Heptadecafluoro-1,1,2,2-tetrahydro-decyl-1-trimethoxysilane (FS) was purchased from Gelest and used as received.

<sup>1</sup>H and <sup>13</sup>C NMR spectra were recorded at room temperature using a 500 MHz Bruker spectrometer, with reference to residual protio solvent (CDCl<sub>3</sub>; δ 7.26 ppm). The data are reported as follows: chemical shifts are reported in ppm on the δ scale, multiplicity (br = broad, s = singlet, d = doublet, t = triplet, q = quartet, m = multiplet). GC-MS was obtained on an Agilent 6890-5973 GC/MS work-station. The GC column was a Hewlett-Packard fused silica capillary column cross-linked with 5% phenylmethylsiloxane, and helium was the carrier gas (1 mL/min). The following conditions were used for all GC/MS analysis: injector and detector temperature, 250 °C; initial temperature, 70 °C; temperature ramp, 10 °C/min; final temperature, 280 °C. Analytical thin layer chromatography was performed on EM reagents 0.25 mm silica gel 60-F plates. Liquid chromatography was performed using flash chromatography of the indicated solvent system on select silica gel (SiO<sub>2</sub>) 230–400 mesh. Molecular weights of the synthesized polymers were measured by size exclusion chromatography (SEC) analysis on a Varian PL-GPC 220 system equipped with Varian PL-Gel Mixed D column (300 mm x 7.5 mm, 5 μm) and Varian PL-Gel guard column (50 mm x 7.5 mm, 5 μm). A GPC solvent/sample module was used with chlorobenzene with 0.0125% BHT as the eluent and the calibrations were based on polystyrene standards. The

running conditions for SEC analysis were as follows: flow rate = 1.0 mL/min, injector volume = 200 μL, detector temperature = 80 °C, column temperature = 80 °C. All the polymer samples were filtered through PTFE filters (0.45 μm) prior to injection. The UV-Vis spectra of polymer solutions in chloroform solvent were carried out in 1 cm cuvettes using an Agilent 8453 UV-Vis spectrometer. Thin films of polymer were obtained by evaporation of chloroform from polymer solutions on glass microscope slides. The films for the determination of absorption coefficients were deposited by spin-casting solutions of 5 mg/mL of polymer in chloroform. Cyclic voltammetry (CV) was done with a BAS CV-50W voltammetric analyzer (Bioanalytical Systems, Inc.). Electrochemical grade tetrabutylammonium perchlorate (TBAP) was used without further purification. Acetonitrile was distilled over calcium hydride and collected over molecular sieves. The electrochemical cell was comprised of a platinum electrode, a platinum wire auxiliary electrode, and an Ag/AgCl reference electrode. Acetonitrile solutions containing 0.1 M TBAP were placed in a cell and purged with argon. A drop of the polymer solution was evaporated on the platinum working electrode in ambient air. The film was immersed into the electrochemical cell containing the electrolyte, and the oxidation potential was observed and recorded. All electrochemical shifts were standardized to the ferrocene redox couples at 0.474 V. X-ray diffraction patterns were obtained on a RIGAKU Ultima III diffractometer. Samples were subjected to Cu-K<sub>α</sub> radiation (λ~1.5406 Å) and scanned from 1 to 40 degrees (2θ) at 0.04° intervals at a rate of 2°/min. A silicon wafer with 200 nm of thermally deposited SiO<sub>2</sub> (22 μm x 22 μm) was used as the sample substrate. The polymer films were deposited in air by drop casting a 5.0 mg/mL polymer/chloroform solution and allowed to dry in a petri dish saturated with chloroform. The devices were then annealed for 30 min at 120 °C. Thermogravimetric analysis (TGA) was done under nitrogen using a Perkin-Elmer Pyris 1 TGA instrument operating from 100 to 600 °C at a heating rate of 10 °C/min. Tapping Mode Atomic Force Microscopy (TMAFM) studies were carried out on a VEECO-dimension 5000 scanning probe microscope with a hybrid xyz head equipped with Nano-Scope Software. AFM images were obtained using silicon cantilevers with nominal spring constant of 42 N/m and nominal resonance frequency of 300 kHz (OTESPa). Image analysis software Nanoscope 7.30 was used for surface imaging and image analysis. All the AFM measurements were conducted under ambient conditions. All cantilever oscillation amplitude were ca. 375 mV, all images were acquired at 2 Hz scan frequency and the sample scan area was 25 μm<sup>2</sup>.

## Field-Effect Mobility Measurements

Field-effect mobility measurements of the synthesized polymers were performed on thin-film transistors with a common bottom-gate, bottom-contact configuration. Highly doped, n-type silicon wafers with a resistivity of 0.001 - 0.003 Ω cm were used as substrates. Silicon dioxide (SiO<sub>2</sub>) was thermally grown at 1000 °C on silicon substrate to obtain a 200 nm thickness. Chromium metal (5 nm) followed by 100 nm of gold was deposited by E-beam evaporation as source-drain contacts. The source-drain pads were formed by photolithographically patterning the metal layer.

The SiO<sub>2</sub> on the backside of the wafer was etched with buffered oxide etchant (BOE from JT Baker) to generate the common bottom-gate. The resulting transistors had a channel width of 475 μm and channel lengths varying from 6 to 80 μm. The measured capacitance density of the SiO<sub>2</sub> dielectric was 17 nF/cm<sup>2</sup> prior to copolymer deposition; the substrates were cleaned under UV/ozone for 10 min. The devices were then cleaned in air with water, methanol, hexane, chloroform, and dried with nitrogen flow followed by vacuum for 30 min at 80 °C. The copolymer films were deposited in air by drop casting 10 μL of a 1.0 mg/mL solution in distilled chloroform and allowed to dry in a petri dish saturated with chloroform. The films cast from chloroform were allowed to dry in air until all the solvent evaporated. The devices were then annealed at 120 °C for 1 hr prior to measurements. A Keithley 4200-SCS semiconductor characterization system and a Cascade microtech model summit microchamber were used to measure the transistors. When measuring the family and transfer curves, V<sub>GS</sub> was scanned from +10 to -65 V. All the measurements were performed in dark at room temperature in air.

### Preparation of Solar Cell Devices

The solar cell substrates were bought from Luminescence Technology Corp. (Taiwan) and were patterned using standard photolithography. The substrates were cleaned by sonication for 20 min in acetone, methanol, toluene, and isopropyl alcohol. The substrates were subjected to UV/ozone treatment for 20 min prior to use. After the ozone treatment, poly(3,4-ethylenedioxythiophene :poly(styrenesulfonate) (PEDOT-PSS) was spin-coated on the substrates (4000 rpm, 1740 rpm/s, 90 s). The substrates were annealed at 120 °C for 10 min under a nitrogen atmosphere. Polymer/PCBM blends were prepared in chloroform with a total blend concentration of 15 mg/mL. These blends were spin-coated (2000 rpm, 60 s) on the PEDOT-PSS treated substrate. Films of 10 nm Ca and 100 nm Al were thermally evaporated on the substrates at a rate of 2.5 Å/s through a shadow mask to obtain the solar cell devices. IV testing was carried out under a controlled nitrogen atmosphere using a Keithley 236, model 9160 interfaced with Lab View software. The solar simulator used was a THERMOORIEL equipped with a 300 W xenon lamp; the intensity of the light was calibrated to 100 mW cm<sup>-2</sup> with a NREL certified Hamamatsu silicon photodiode. The active area of the devices was 0.1 cm<sup>2</sup>. The active layer film thickness was measured using a Veeco Dektak VIII profilometer.

### Space Charge Limited Current Measurements

ITO substrates were prepared in a similar fashion to those used for the solar cell devices. After the ozone treatment, PEDOT-PSS was spin-coated on the substrates (4000 rpm, 1740 rpm/s, 90 s). The substrates were annealed at 150 °C for 10 min under a nitrogen atmosphere. Concentrated polymer solutions (15 mg/mL) were prepared in chloroform and were spin-coated (2000 rpm, 60 s) on to the PEDOT-PSS treated substrate. Al (100 nm) was thermally evaporated on to the substrates at a rate of 2.75 Å/s through a shadow mask to form a Schottky junction. IV testing was carried out under a controlled nitrogen atmosphere using a Keithley 236, model 9160 interfaced with LabView software. The active area of the devices was 0.1 cm<sup>2</sup>. The active layer film

thickness was measured using a Veeco Dektak VIII profilometer.

## Experimental

### GRIM Polymerization of 2,6-dibromo-4,8-bis(5-dodecylthiophene-2-yl)benzo[1,2-*b*:4,5-*b'*]dithiophene (P1)

A dry three-neck flask was flushed with nitrogen and was charged with *n*-BuLi (0.3 mmol, 2.5 M in hexanes) and a solution of *n*-BuMgCl (0.15 mmol, 2 M in THF) in dry toluene (2 mL) at 0 °C. Meanwhile a solution of di-brominated monomer (0.089 g, 0.105 mmol) in anhydrous THF was bubbled with nitrogen for 15-20 minutes. At -78 °C the prepared monomer solution was added to the ate-complex and the reaction mixture was stirred for 1 hr. Monomer conversion was determined by using <sup>1</sup>H NMR. The color changed to dark green from yellow. Ni(dppp)Cl<sub>2</sub> (0.006 g, 0.01 mmol) was added to the reaction mixture at room temperature. The polymerization was allowed to proceed overnight at room temperature; followed by quenching the reaction in a mixture of methanol (200 mL) and HCl (~20 mL). A red colored precipitate was obtained. The precipitated polymer was filtered through a thimble and was purified by Soxhlet extractions using methanol, diethyl ether, hexanes, and chloroform successively, with drying in between extractions. The product was red solid (0.04 g, 55.0%). <sup>1</sup>H NMR (CDCl<sub>3</sub>, 500 MHz), δ: 0.89 (br, 6H), 1.380 (br, 40H), 2.90 (br, 4H), 7.02 (br, 6H), SEC: M<sub>n</sub> = 6700 g mol<sup>-1</sup>, PDI = 1.30.

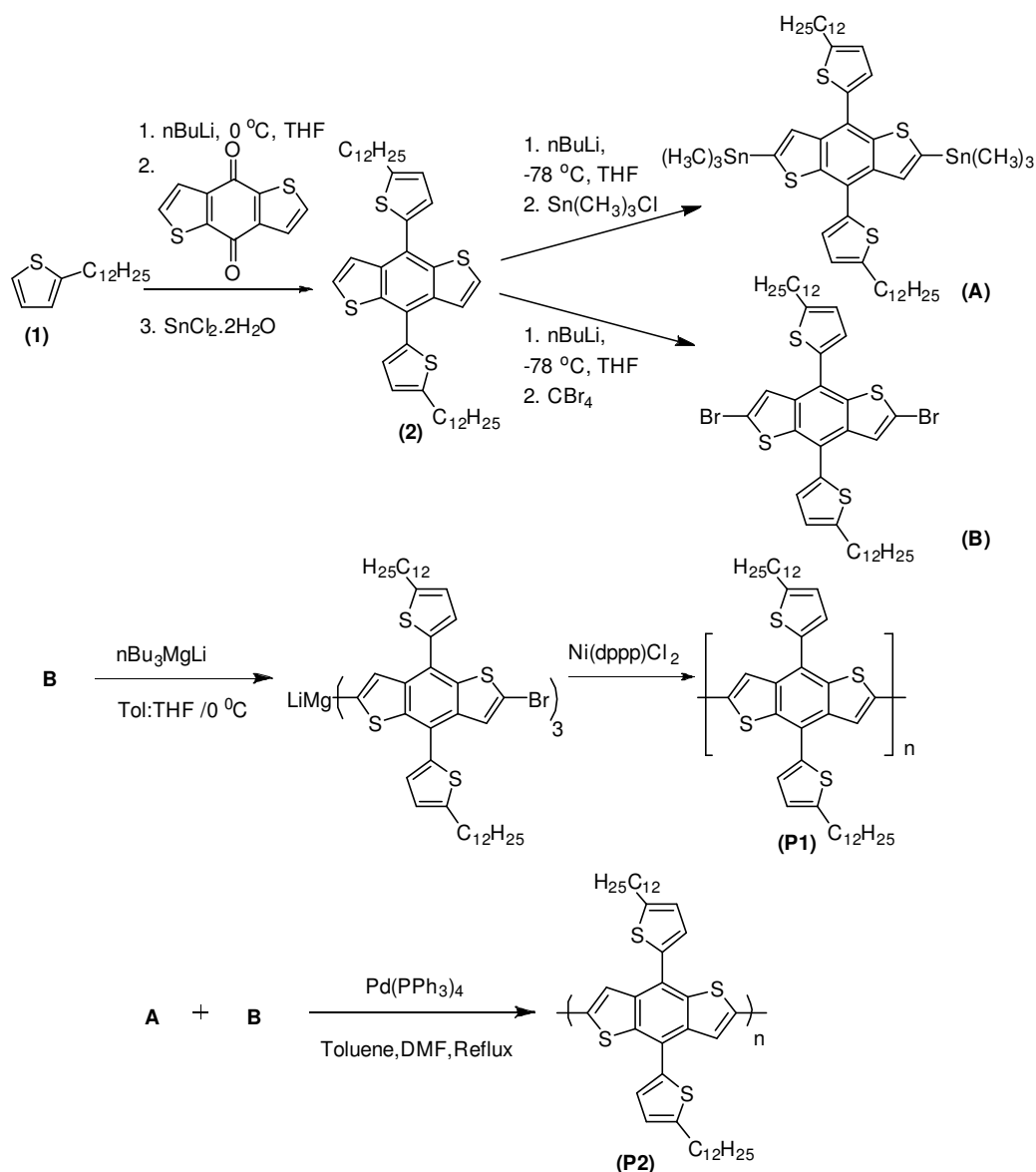
### Stille coupling polymerization of 4,8-bis(5-dodecylthiophene-2-yl)benzo[1,2-*b*:4,5-*b'*]dithiophene (P2)

2,6-Dibromo-4,8-bis(5-dodecylthiophene-2-yl)benzo[1,2-*b*:4,5-*b'*]dithiophene (0.31 g, 0.365 mmol), 2,6-(trimethyltin)-4,8-bis(5-dodecylthiophene-2-yl)benzo[1,2-*b*:4,5-*b'*]dithiophene (0.37 g, 0.365 mmol), and tetrakis(triphenylphosphine) palladium(0) (7.31 mg, 0.0072 mmol) were added to a three neck round bottom flask under a nitrogen atmosphere and they were dissolved in a mixture of toluene (30 mL) and DMF (0.5 mL). The solution was heated at reflux for 24 hr before precipitating the polymer in a mixture of methanol (200 mL) and HCl (20 mL). The polymer was filtered and purified by Soxhlet extraction with methanol, diethyl ether, hexanes, dichloromethane, and chloroform successively. The polymer was obtained from the chloroform fraction upon evaporation of the solvent. The product was a red solid (0.23 g, 90.0%). <sup>1</sup>H NMR (CDCl<sub>3</sub>, 500 MHz), δ: 0.89 (br, 6H), 1.380 (br, 40H), 2.90 (br, 4H), 7.02 (br, 6H), SEC: M<sub>n</sub> = 25470 g mol<sup>-1</sup>, PDI = 3.71.

## Results and Discussion

### Synthesis and Characterization

We recently reported the synthesis of homopolymers of BDT with phenylethynyl substituents using the GRIM polymerization.<sup>14, 16, 36</sup> However, the coordination of Ni in to the ethynyl linkage hindered the GRIM polymerization and low molecular weights were obtained. Moreover due to the electron withdrawing nature of the ethynyl linkage, the homopolymers of BDT with phenylethynyl substituents did not show desirable optoelectronic properties as well. As such, to prevent the loss of Ni catalytic activity through coordination with the ethynyl linkages and to gain better optoelectronic properties



**Scheme 1.** Synthesis of poly{4,8-bis(5-dodecylthiophene-2-yl)benzo[1,2-b:4,5-b']dithiophene} using Grignard metathesis polymerization (**P1**) and Stille coupling polymerization (**P2**)

and solubility in common organic solvents, electron-donating alkylthienyl substituents were attached at the 4- and 8- positions of BDT core, which was utilized in GRIM polymerization and in Stille coupling polymerization methods. The general synthetic routes of the synthesis of the monomers and polymers are outlined in Scheme 1, and the synthetic procedures for the synthesis of monomers are included in supporting information.

The polymer (**P1**) was synthesized via GRIM polymerization of 2,6-dibromo-4,8-bis(5-dodecylthiophene-2-yl)benzo[1,2-b:4,5-b']dithiophene. The first step, the magnesium-halogen exchange step in the GRIM polymerization is typically accompanied by reaction of the aryl bromide with *t*-BuMgCl or *i*-PrMgCl. Treatment of 2,6-dibromo-4,8-bis(5-dodecylthiophene-2-yl)benzo[1,2-b:4,5-b']dithiophene with 1 equivalent of RMgCl (R = alkyl) should result in a magnesium-bromine exchange reaction, also referred to as the Grignard metathesis (GRIM); however, due to the bulkiness of the monomer the metal-halogen exchange gave a

low yield. As such the bulky aryl bromide was reacted in the presence of magnesium-ate complex to achieve a better yield for the metal halogen exchange reaction. The monomer conversion was monitored using  $^1\text{H}$  NMR and after the monomer was reacted to generate the 2-bromo-6-magnesio-4,8-bis(5-dodecylthiophene-2-yl)benzo[1,2-b:4,5-b']dithiophene the Ni(II) catalyst was added to obtain the homopolymer **P1**. The polymer **P2** was synthesized via Stille coupling polymerization of 2,6-dibromo-4,8-bis(5-dodecylthiophene-2-yl)benzo[1,2-b:4,5-b']dithiophene and 2,6-bis(trimethyltin)-4,8-bis(5-dodecylthiophene-2-yl)benzo[1,2-b:4,5-b']dithiophene in the presence of tetrakis(triphenylphosphine) palladium(0) as the catalyst. The synthesized polymers were purified by Soxhlet extractions with methanol, hexanes, diethyl ether, and chloroform respectively, with successive drying after each extraction. The final purified polymer was obtained by the evaporation of the chloroform fraction.

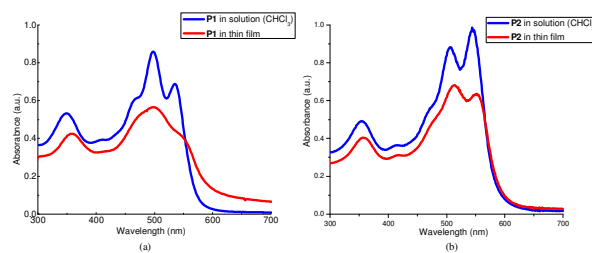
**Table 1** Optoelectronic properties and molecular weights of the synthesized polymers **P1** and **P2**

Polymer	$M_n^a$ (g/mol)	PDI <sup>a</sup>	$\lambda_{max}^b$ (nm)	$\lambda_{max}^c$ (nm)	HOMO <sup>d</sup> (eV)	LUMO <sup>d</sup> (eV)	$E_g^e$ (eV)
<b>P1</b>	6700	1.30	348, 497, 535	358, 498, 552	-5.26	-2.87	-2.39
<b>P2</b>	25470	3.70	354, 504, 545	360, 513, 554	-5.25	-2.87	-2.38

<sup>a</sup> Determined by SEC (chlorobenzene eluent), <sup>b</sup> Absorption maxima of chloroform solution, <sup>c</sup> Absorption maxima of thin films, <sup>d</sup> Estimated from the onset of reduction wave of cyclic voltammograms,  $E_g = (LUMO^e - HOMO^d)$

The obtained copolymers from chloroform were readily soluble in common organic solvents such as chlorobenzene, tetrahydrofuran, dichlorobenzene, and chloroform and produced deep red solutions. Size exclusion chromatography results (using polystyrene as the standard and chlorobenzene as the eluent) have shown that the polymers **P1** and **P2** had number average molecular weight ( $M_n$ ) values ranging from 6.7 to 25 kDa, respectively (Table 1). It was observed that the use of GRIM polymerization resulted in a polymer with a very narrow PDI of 1.30 for the polymer **P1**, whereas a very broad PDI of 3.70 was observed for the polymer **P2** generated from Stille coupling polymerization. Both polymers were characterized by <sup>1</sup>H NMR spectra (Fig. S1-S6 in Supporting Information). Both polymers **P1** and **P2** showed comparable <sup>1</sup>H NMR spectra with a broad peak at 7.02 ppm in the aromatic region indicating aggregation of the polymers in deuterated solvents.

The UV-Vis absorption spectra of the two polymers **P1** and **P2** were recorded in chloroform solutions and in thin films (Fig. 1). Both the polymers showed three absorbance maxima in the solution as well as in films, with one in the UV region (**P1**,  $\lambda_{max} = 348$  nm; **P2**,  $\lambda_{max} = 354$  nm) and two in the visible region (**P1**,  $\lambda_{max} = 497$  nm,  $\lambda_{max} = 535$  nm; **P2**,  $\lambda_{max} = 504$  nm,  $\lambda_{max} = 545$  nm) (Fig. 1, Table 1). The absorbance maxima observed in the UV region was due to the conjugation along the side chain of the benzodithiophene unit.<sup>16,24</sup> The strong absorbance maxima observed in the visible region,  $\lambda_{max} = 497$  nm for **P1** and  $\lambda_{max} = 504$  nm for **P2**, was attributed to the  $\pi-\pi^*$  transition between the benzodithiophene units in the polymer backbone. Both the polymers showed vibronic peaks as well;  $\lambda_{max} = 535$  nm for polymer **P1** and  $\lambda_{max} = 545$  nm for polymer **P2**. The intensity of the absorbance due to the conjugation along the polymer backbone and the absorbance due to the side chains reflects the relative ratio in the repeating units.<sup>16,24</sup> As such, the polymer **P2** has a higher repeating units ratio due to the larger molecular weight of the polymer compared to that of the polymer **P1**. Both the polymers **P1** and **P2** showed a red-shift (~20 nm for polymer **P1** and ~10 nm for polymer **P2**) in absorption bands of the thin films compared to that of the solutions. This indicates more structural organization and ordered packing which enhanced the aggregation of the polymer in thin films compared to that of the solution. Although the polymer **P2** had higher molecular

**Fig.1** UV-Vis absorption spectra of polymer **P1** (left) and polymer **P2** (right): red, film; blue, solution (chloroform solvent)

weight and hence a larger conjugation length compared to that of the polymer **P1**, UV/Vis spectra of the polymers in solution as well as in thin films are almost the same. This indicates that the effective conjugation length of the poly{4,8-bis(5-dodecylthiophene-2-yl)benzo[1,2-*b*:4,5-*b'*]dithiophene} is closer to the conjugation length of the polymer **P1**, implying that after 10-15 repeat units of thienyl substituted BDT, the optical, electrochemical and other physical properties of poly{4,8-bis(5-dodecylthiophene-2-yl)benzo[1,2-*b*:4,5-*b'*]dithiophene} will reach its saturation level.<sup>38</sup>

Fluorescence spectra of the polymers have been recorded in chloroform solutions (Fig. S8, S9 in Supporting Information). Both polymers displayed similar fluorescence spectra and both displayed an emission peak at 586 nm upon excitation at 355 nm.

HOMO and LUMO energy levels of the polymers **P1** and **P2** were estimated by using cyclic voltammetry using the onset of oxidation and reduction potentials, respectively (Fig. S10 in Supporting Information). The HOMO and the LUMO energy levels of polymer **P1** were determined as -5.26 eV and -2.87 eV, and those of the polymer **P2** as -5.25 eV and -2.87 eV, respectively (Table 1). Both polymers **P1** and **P2** had a band gap of ~2.39 eV. The HOMO energy levels of polymers **P1** and **P2** are similar to the air oxidation threshold (ca. -5.27 eV), indicating good air stability for both the polymers **P1** and **P2**. Although the polymer **P2** has a higher molecular weight and hence a higher conjugation compared to polymer **P1**, the HOMO and LUMO energy levels and thus the band gap of the polymers, were comparable. This further aid the assumption that the effective conjugation length of the poly{4,8-bis(5-dodecylthiophene-2-yl)benzo[1,2-*b*:4,5-*b'*] dithiophene} is closer to the conjugation length of polymer **P1**, as such the polymer **P2** may not experience additional orbital overlapping and hence the HOMO, LUMO energy levels and the band gap of the polymers are the same.<sup>38</sup>

The thermal stability of the two polymers **P1** and **P2** were estimated using thermo gravimetric analysis, which was performed under a nitrogen atmosphere with a heating rate of 10 °C/min (Fig. S7 in Supporting Information). The onset of decomposition for the two polymers similar and was around 400 °C, indicating good thermal stability for the two polymers.

The field-effect mobilities of polymers **P1** and **P2** were measured in bottom-gate, bottom-contact organic field-effect transistors (OFETs).  $I_{DS}-V_{DS}$  family curves and  $I_{DS}-V_{GS}$  transfer curves were recorded. The charge carrier mobility was extracted by plotting  $I_{DS}^{1/2}$  vs.  $V_{GS}$  the saturation regime, using the following equation,

$$\mu_{sat} = \frac{2L}{WC_i} m^2$$

$\mu$  is the mobility obtained in the saturation regime,  $L$  is the channel length,  $W$  is the channel width,  $C_i$  is the capacitance of the dielectric, and  $m$  is the slope of the  $I_{DS}^{1/2}$  vs.  $V_{GS}$  in the saturation regime.

**Table 2.** Field effect mobilities, Threshold voltages, and On/Off ratios of polymers **P1** and **P2** measured on bottom-gate bottom-contact OFETs

Polymer	Surface treatment	Mobility ( $\text{cm}^2/\text{Vs}$ ) <sup>a</sup>	$I_{on}/I_{off}$	$V_T$ (V)
<b>P1</b>	-	$1.82 \times 10^{-7}$ ( $1.15 \times 10^{-7}$ )	$3.70 \times 10^1$	-65.3
	FS treated	$4.20 \times 10^{-5}$ ( $3.40 \times 10^{-5}$ )	$1.00 \times 10^2$	-26.8
<b>P2</b>	-	$1.40 \times 10^{-6}$ ( $0.95 \times 10^{-6}$ )	$1.20 \times 10^1$	-37.1
	FS treated	$4.61 \times 10^{-4}$ ( $2.30 \times 10^{-4}$ )	$5.10 \times 10^2$	-12.8

<sup>a</sup> Field effect mobilities represents the largest measured values and the numbers listed in parenthesis represent average values.

The field-effect mobilities of both polymers were measured on both untreated and silane-treated OFET devices. Polymer **P1** exhibited a mobility of  $1.82 \times 10^{-7} \text{ cm}^2/(\text{Vs})$  and polymer **P2** exhibited a mobility of  $1.4 \times 10^{-6} \text{ cm}^2/(\text{Vs})$  on an untreated OFET devices (Table 2). The device performances of OFETs could be enhanced by lowering the surface energy of the interaction between the semiconducting polymer and the gate dielectric. We have previously reported that the field-effect mobilities of benzodithiophene based polymers could be enhanced upon the treatment of the surface of  $\text{SiO}_2$  dielectric with hydrophobic heptadecafluoro-1,1,2,2-tetrahydro-decyl-1-trimethoxysilane.<sup>39</sup> As such in this study heptadecafluoro-1,1,2,2-tetrahydro-decyl-1-trimethoxysilane (FS) was used for the surface treatment of silicon dioxide dielectric. The measured field-effect mobilities of polymer **P1** on treated devices were  $4.20 \times 10^{-5} \text{ cm}^2/(\text{Vs})$  (Fig. 2) and that for the polymer **P2** on treated devices was  $4.61 \times 10^{-4} \text{ cm}^2/(\text{Vs})$  (Fig. 3). Mobilities of both the polymers **P1** and **P2** increased upon the treatment of FS because FS facilitated higher interaction between hydrophobic  $\text{SiO}_2$  dielectric and the hydrophobic polymer. Although the molecular weight of the polymer **P2** was higher than that of the polymer **P1** by 3 folds, it should be noted that the charge carrier mobility of polymer **P2** was only improved by one order of magnitude compared to that of the polymer **P1**. The hole-carrier transportation in OFETs occurs horizontally as such the extent of conjugation, better packing and long range order facilitates the charge transport. The smaller increase in charge carrier mobility of the polymer **P2** in comparison to the polymer **P1** despite its larger molecular weight may be due to the broader PDI (3.70) of the polymer **P2**. A broader PDI indicates the presence of low molecular weight polymer chains and oligomers, which can act as charge carrier traps to affect the overall charge carrier mobility in OFETs.

Thin film X-ray diffraction patterns were obtained for both polymers **P1** and **P2** (Fig. 4). In each case, the patterns lacked the intense narrow peaks that would indicate a high degree of crystallinity. Instead, the profiles displayed broad peaks at  $2\theta = 2.7^\circ$  and  $19.3^\circ$  for **P1**, and  $2\theta = 2.9^\circ$  and  $22.8^\circ$  for **P2**. The peaks at  $2.7^\circ$  and  $2.9^\circ$ , which correspond to d-spacing of  $33.1 \text{ \AA}$  and  $30.1 \text{ \AA}$  for **P1** and **P2** respectively, indicate a small degree of

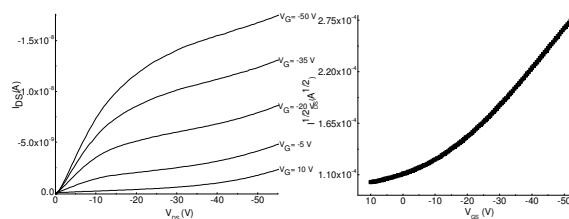


**Fig. 2** Current-voltage characteristics of polymer **P1** on FS-treated OFET: output curves at different gate voltages (left) and transfer curve at  $V_{DS} = -55 \text{ V}$  ( $\mu = 4.20 \times 10^{-5} \text{ cm}^2/(\text{Vs})$ ,  $V_T = 26.8 \text{ V}$ , On/Off =  $1.00 \times 10^2$ ) (right) ( $W = 475 \text{ }\mu\text{m}$ ,  $L = 20 \text{ }\mu\text{m}$ )

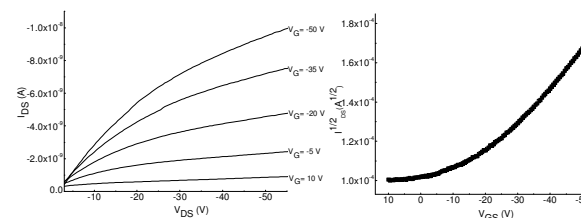


**Fig. 3** Current-voltage characteristics of polymer **P2** on FS-treated OFET: output curves at different gate voltages (left) and transfer curve at  $V_{DS} = -55 \text{ V}$  ( $\mu = 4.20 \times 10^{-5} \text{ cm}^2/(\text{Vs})$ ,  $V_T = 26.8 \text{ V}$ , On/Off =  $1.00 \times 10^2$ ) (right) ( $W = 475 \text{ }\mu\text{m}$ ,  $L = 20 \text{ }\mu\text{m}$ )

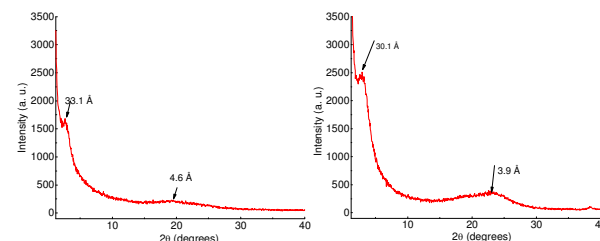


**Fig. 4** Thin film XRD patterns of polymer **P1** (left) and polymer **P2** (right) on  $\text{SiO}_2$  substrate deposited from chloroform.

lamellar ordering of adjacent polymer strands. The broad peaks centered around  $19.3^\circ$  and  $22.8^\circ$  were assigned to  $\pi$ -stacking distances of  $4.6 \text{ \AA}$  and  $3.9 \text{ \AA}$  between benzodithiophene moieties of parallel polymer chains.

**Table 3** Photovoltaic properties of Polymers **P1** and **P2**

Polymer	[P]:[PC <sub>71</sub> BM]	$V_{oc}$ (V)	$J_{sc}$ ( $\text{mA}/\text{cm}^2$ )	FF	PCE (%)
<b>P1</b>	1:1	0.31 (0.30)	4.87 (4.69)	0.37 (0.30)	0.57 (0.43)
	1:2	0.64 (0.61)	3.61 (3.63)	0.30 (0.31)	0.69 (0.69)
	1:3	0.82 (0.73)	4.06 (3.74)	0.39 (0.33)	1.32 (0.92)
	1:4	0.72 (0.70)	3.62 (3.46)	0.38 (0.33)	0.99 (0.81)
	1:1	0.75 (0.73)	3.34 (3.42)	0.34 (0.33)	0.85 (0.82)
<b>P2</b>	1:2	0.75 (0.73)	3.69 (3.82)	0.36 (0.33)	1.01 (0.94)
	1:3	0.76 (0.76)	3.63 (3.60)	0.41 (0.40)	1.14 (1.10)
	1:4	0.75 (0.73)	3.18 (3.21)	0.37 (0.35)	0.89 (0.83)

Data in the parenthesis represents the average measured PCE values

The photovoltaic properties of the polymers were investigated in bulk heterojunction (BHJ) solar cells using the conventional solar cell device structure of ITO/PEDOT:PSS/polymer: PC<sub>71</sub>BM/Ca/Al and were tested under 1.5 AMG illuminations. The polymer PC<sub>71</sub>BM blends were prepared in chloroform at a concentration of 15 mg/mL for the both polymers, **P1** and **P2**. The optimal blending ratio for the polymers was determined by testing the polymers in BHJ solar cell by varying [P]:[PCBM] weight ratio from 1:1 to 1:4 (Table 3). For both the polymers, the PCEs increased with increasing PCBM content from 1:1 to 1:3, with an optimal blending ratio of 1:3 (Fig. 5). The PCE of polymer **P1** increased from 0.57% to 1.32%, with an increase in the open circuit voltage from 0.31 V to 0.82 V and an increase in the fill factor from 0.37 to 0.39. The PCE of polymer **P2** increased from 0.85% to 1.14%, with an increase in the fill factor from 0.34 to 0.41 (Table 3). However for both the polymers a significant change was not observed in the short circuit current density upon increasing the PC<sub>71</sub>BM weight ratio.

For the polymer **P1**;  $J_{SC}$  was  $\sim 4.00$  mA/cm<sup>2</sup> and for the polymer **P2**;  $J_{SC}$  of  $\sim 3.6$  mA/cm<sup>2</sup> was measured. Although the polymer **P2** had a higher molecular weight compared to **P1**, the PCE of the polymer **P1** was higher than that of polymer **P2**. This was attributed to the broader PDI observed for the polymer **P2**. A broader PDI indicated the presence of low molecular weight chains, oligomers, unreacted or deactivated monomers, and cross coupling by-products. These organic impurities may decrease the charge carrier mobilities and can act as traps in the active layer, thereby increasing the probability of charge recombination.<sup>30</sup> Moreover it has been found that these organic impurities can diffuse to the interface between the active layer and the cathode and react with the metal cathode.<sup>29</sup> These factors may decrease the  $J_{SC}$  and hence the PCE of the polymer. Thus the lower PDI = 1.3 of polymer **P1** appears to be beneficial for the  $J_{SC}$  and hence the higher PCE in solar cell devices.

The vertical hole-carrier transport behaviour of the polymers **P1** and **P2** was investigated by using the space charge limited current (SCLC) model in which a device structure of ITO/PEDOT:PSS/polymer/Al was employed (Fig. 6). The following equation was used for the calculations of the charge carrier mobilities of the polymers,

$$J = 9\epsilon_0\epsilon_r\mu\frac{V^2}{8L^3}$$

where  $J$  is the current density,  $\epsilon_0\epsilon_r$  is the permittivity of the polymer,  $\mu$  is the charge carrier mobility, and  $L$  is the active layer thickness. The mobility was extracted by taking the slope of a  $J$  vs.  $V^2$  plot in the space-charge limited regime (taken as voltages greater than 400 mV) and solving for mobility. The polymer **P1** showed higher charge carrier mobility of  $1.88 \times 10^{-5}$  cm<sup>2</sup> V<sup>-1</sup> s<sup>-1</sup>, and **P2** showed a mobility of  $3.41 \times 10^{-6}$  cm<sup>2</sup> V<sup>-1</sup> s<sup>-1</sup>. These results are consistent with that of the solar cell data in which the higher efficiency was observed for the polymer **P1**.

Tapping-mode atomic force microscopy (TMAFM) of both polymers **P1** and **P2** were performed on thin films in channel regions between the source-drain electrodes on OFET devices (Fig.7). TMAFM analyses were carried out on the same devices which were used for the mobility measurements. Both polymers

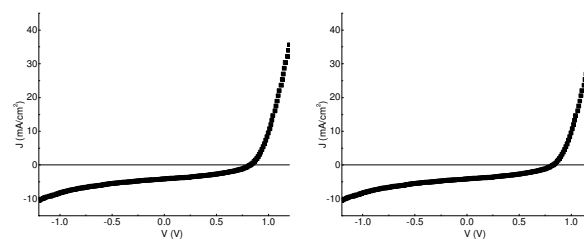


Fig. 5 I-V curves of the polymers **P1** (left) and **P2** (right).

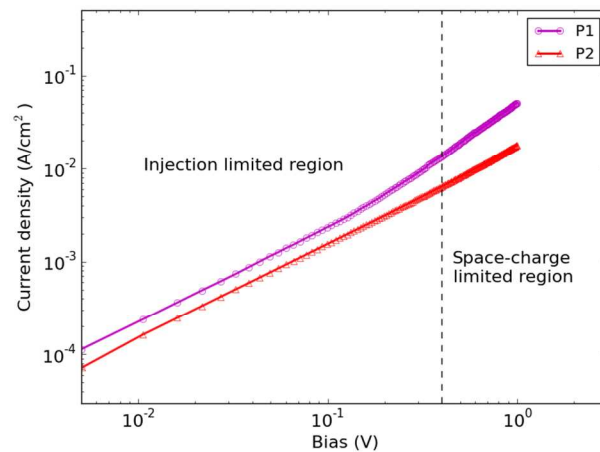


Fig. 6 Current density and voltage curves of polymer **P1** (purple) and polymer **P2** (red)

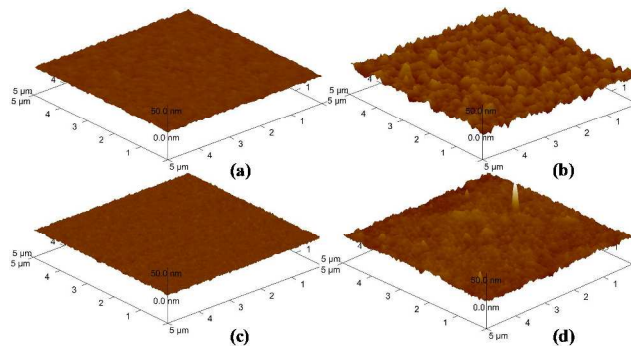


Fig. 7 3D height TMAFM images of thin films of polymer **P1** measured in the channel between the source-drain electrodes on: (a) untreated OFET device (b) FS-treated OFET device; polymer **P2** measured in the channel between the source-drain electrodes on: (c) untreated OFET device (d) FS-treated OFET device

**P1** and **P2** displayed a granular morphology. The FS-treated SiO<sub>2</sub> of polymer **P1** presented a relatively rough surface, compared to FS treated SiO<sub>2</sub> of polymer **P2**. Thickness of the semiconducting polymer films can vary due to the roughness of the SiO<sub>2</sub> interface which results uneven surface. Also, increased roughness of the interface could lead to valleys in the channel region, which could act as carrier traps.<sup>40</sup> Consequently polymer **P2** shows better field-effect mobilities than polymer **P1**, indicating that a smooth hydrophobic surface generates a better interface between the polymer and the SiO<sub>2</sub> dielectric surface.

## Conclusions

Polymerization of 2,6-dibromo-4,8-bis(5-dodecylthiophene-2-yl)benzo[1,2-*b*:4,5-*b'*]dithiophene has been achieved through

GRIM polymerization and through Stille coupling polymerization. The Stille coupling polymerization generated a polymer (**P2**) with a comparatively larger molecular weight and a broader PDI, whereas the GRIM polymerization generated a polymer (**P1**) with a lower molecular weight and a narrow PDI. The optoelectronic properties of the polymers are comparable due to the fact that the effective conjugation length the poly{4,8-bis(5-dodecylthiophene-2-yl)benzo[1,2-*b*:4,5-*b'*]dithiophene} is closer to the conjugation length of the polymer **P1**. The broader PDI of the polymer **P2** had detrimental effect on OPV performances and in SCLC performances and the charge carrier mobility of the polymer **P2** in OFETs was only one order of magnitude higher than that of the polymer **P1**.

## Notes and references

<sup>15</sup> <sup>a</sup>Department of Chemistry, University of Texas at Dallas, 800 West Campbell Road, Richardson, TX 75080, USA.

\*Corresponding author Email address: [mihaela@utdallas.edu](mailto:mihaela@utdallas.edu)

<sup>b</sup>Department of Materials Science and Engineering, University of Texas at Dallas, 800 West Campbell Road, Richardson, Texas 75080, USA.

<sup>20</sup> <sup>c</sup>Plextronics, Inc, 2180 WilliamPitt Way, Pittsburgh, PA 15238, USA.

† Electronic Supplementary Information (ESI) available: [details of any supplementary information available should be included here]. See DOI: 10.1039/b000000x/ *Electronic Supplementary Information (ESI) available: [details of any supplementary information available should be included here]. See DOI: 10.1039/b000000x/*

- I. F. Perepichka and D. F. Perepichka, *Handbook of Thiophene-based Materials: Applications in Organic Electronics and Photonics, Volume One: Synthesis and Theory*, **2009**.
- T. A. Skotheim and J. Reynolds, *Handbook of Conducting Polymers*, CRC Press, LLC, Boca Raton, **2006**.
- A. Facchetti, *Chemistry of Materials*, **2011**, *23*, 733-758.
- E. Zhou, S. Yamakawa, K. Tajima, C. Yang and K. Hashimoto, *Chem. Mater.* **2009**, *21*, 4055-4061.
- J. Chen and Y. Cao, *Acc. Chem. Res.* **2009**, *42*, 1709-1718.
- A. J. Heeger, *Chem. Soc. Rev.* **2010**, *39*, 2354-2371.
- T.-A. Chen, X. Wu and R. D. Rieke, *J. Am. Chem.Soc.* **1995**, *117*, 233-244.
- R. D. McCullough, *Adv. Mater.* **1998**, *10*, 93-116.
- P. Sista, M. C. Biewer and M. C. Stefan, *Macromol. Rapid Commun.*, **2012**, *33*, 9-20.
- E. Bundgaard and F. C. Krebs, *Sol. Energy Mater. Sol.Cells*, **2007**, *91*, 954-985.
- R. S. Kularatne, H. D. Magurudeniya, P. Sista, M. C. Biewer and M. C. Stefan, *J.Polym.Sci. Part A: Polym. Chem.* **2012**, *51*, 743-768.
- J. Hou, H.-Y. Chen, S. Zhang and Y. Yang, *J. Phys. Chem. C*, **2009**, *113*, 21202-21207.
- Y. Li, *Acc. Chem. Res.* **2012**, *45*, 723-733.
- N. Hundt, K. Palaniappan, J. Servello, D. K. Dei, M. C. Stefan and M. C. Biewer, *Org. Lett.*, **2009**, *11*, 4422-4425.
- Z. Gu, P. Shen, S.-W. Tsang, Y. Tao, B. Zhao, P. Tang, Y. Nie, Y. Fang and S. Tan, *Chem. Commun.* **2011**, *47*, 9381-9383.
- P. Sista, H. Nguyen, J. W. Murphy, J. Hao, D. K. Dei, K. Palaniappan, J. Servello, R. S. Kularatne, B. E. Gnade, B. Xue, P. C. Dastoor, M. C. Biewer and M. C. Stefan, *Macromolecules* **2010**, *43*, 8063-8070.
- S. Xiao, A. C. Stuart, S. Liu and W. You, *ACS App. Mater. & Interfaces*, **2009**, *1*, 1613-1621.
- M. Yuan, A. H. Rice and C. K. Luscombe, *J.Polym.Sci. Part A: Polym. Chem.* **2011**, *49*, 701-711.
- G. Zhang, Y. Fu, Z. Xie and Q. Zhang, *Polymer*, **2011**, *52*, 415-421.
- G. Zhang, Y. Fu, Q. Zhang and Z. Xie, *Macromol. Chem. Phys.*, **2010**, *211*, 2596-2601.
- G. Zhang, Y. Fu, Q. Zhang and Z. Xie, *Chem. Commun.* **2010**, *46*, 4997-4999.
- S. C. Price, A. C. Stuart, L. Yang, H. Zhou and W. You, *J. Am. Chem. Soc.* **2011**, *133*, 4625-4631.
- R. S. Kularatne, P. Sista, H. Q. Nguyen, M. P. Bhatt, M. C. Biewer and M. C. Stefan, *Macromolecules*, **2012**, *45*, 7855-7862.
- P. Sista, R. S. Kularatne, M. E. Mulholland, M. Wilson, N. Holmes, X. Zhou, P. C. Dastoor, W. Belcher, S. C. Rasmussen, M. C. Biewer and M. C. Stefan, *J.Polym.Sci. Part A: Polym. Chem.*, **2013**, *51*, 2622-2630.
- L. Huo, X. Guo, S. Zhang, Y. Li and J. Hou, *Macromolecules*, **2011**, *44*, 4035-4037.
- R. S. Kularatne, F. J. Taenzler, H. D. Magurudeniya, J. Du, J. W. Murphy, E. E. Sheina, B. E. Gnade, M. C. Biewer and M. C. Stefan, *J.Mater. Chem. A*, **2013**, *1*, 15535-15543.
- Z. He, C. Zhong, S. Su, M. Xu, H. Wu and Y. Cao, *Nat Photon*, **2012**, *6*, 591-595.
- J. Yuan, X. Huang, F. Zhang, J. Lu, Z. Zhai, C. Di, Z. Jiang and W. Ma, *J.Mater.Chem.* **2012**, *22*, 22734-22742.
- W. R. Mateker, J. D. Douglas, C. Cabanetos, I. T. Sachs-Quintana, J. A. Bartelt, E. T. Hoke, A. El Labban, P. M. Beaujuge, J. M. J. Frechet and M. D. McGehee, *Energy. Environ. Sci.* **2013**, *6*, 2529-2537.
- W. L. Leong, G. C. Welch, L. G. Kaake, C. J. Takacs, Y. Sun, G. C. Bazan and A. J. Heeger, *Chem. Sci.* **2012**, *3*, 2103-2109.
- M. C. Iovu, E. E. Sheina, R. R. Gill and R. D. McCullough, *Macromolecules*, **2005**, *38*, 8649.
- R. D. McCullough and R. D. Lowe, *J. Chem. Soc., Chem. Commun.*, **1992**, 70-72.
- M. Verswyvel, C. Hoebbers, J. De Winter, P. Gerbaux and G. Koeckelberghs, *J.Polym. Sci. Part A: Polym. Chem.* **2013**, *51*, 5067-5074.
- C. R. Bridges, T. M. McCormick, G. L. Gibson, J. Hollinger and D. S. Seferos, *J.Am. Chem. Soc.* **2013**, *135*, 13212-13219.
- M. C. Stefan, M. P. Bhatt, P. Sista and H. D. Magurudeniya, *Polym.Chem.* **2012**, *3*, 1693-1701.
- H. D. Magurudeniya, P. Sista, J. K. Westbrook, T. E. Ourso, K. Nguyen, M. C. Maher, M. G. Alemseghed, M. C. Biewer and M. C. Stefan, *Macromol. Rapid Commun.*, **2011**, *32*, 1748-1752.
- P. Beimling and G. Kobmehl, *Chem. Ber.*, **1986**, *119*, 3198-3203.
- P. Salvatori, E. Mosconi, E. Wang, M. Andersson, M. Muccini and F. De Angelis, *J. Phys. Chem. C*, **2013**, *117*, 17940-17954.
- P. Sista, M. P. Bhatt, A. R. McCary, H. Nguyen, J. Hao, M. C. Biewer and M. C. Stefan, *J. Polym. Sci., Part A: Polym. Chem.*, **2011**, *49*, 2292-2302.
- J. Veres, S. Ogie, G. Lloyd and D. de Leeuw, *Chem. Mater.* **2004**, *16*, 4543-4555.